Supramolecular Chemistry
Publication details, including instructions for authors and subscription information:
http://www.informaworld.com/smpp/title~content=t713649759

Supramolecular helix and β-sheet through self-assembly of two isomeric tetrapeptides in crystals and formation of filaments and ribbons in the solid state

Arpita Dutta[a]; Anita Dutt[a]; Michael G. B. Drew[b]; Animesh Pramanik[a]
[a] Department of Chemistry, University of Calcutta, Kolkata, India [b] School of Chemistry, The University of Reading, Reading, UK

To cite this Article Dutta, Arpita , Dutt, Anita , Drew, Michael G. B. and Pramanik, Animesh(2008) 'Supramolecular helix and β-sheet through self-assembly of two isomeric tetrapeptides in crystals and formation of filaments and ribbons in the solid state', Supramolecular Chemistry, 20: 7, 625 — 633
To link to this Article: DOI: 10.1080/10610270701565194
URL: http://dx.doi.org/10.1080/10610270701565194

Supramolecular Chemistry
Vol. 20, No. 7, October–November 2008, 625–633

Taylor & Francis
Taylor & Francis Group

Supramolecular helix and β-sheet through self-assembly of two isomeric tetrapeptides in crystals and formation of filaments and ribbons in the solid state

Arpita Dutta[a], Anita Dutt[a], Michael G. B. Drew[b] and Animesh Pramanik[a]*

[a]*Department of Chemistry, University of Calcutta, 92, A. P. C. Road, Kolkata 700 009, India;* [b]*School of Chemistry, The University of Reading, Whiteknights, Reading RG6 6AD, UK*

(*Received 23 April 2007; final version received 9 July 2007*)

Single crystal X-ray diffraction studies show that the β-turn structure of tetrapeptide I, Boc-Gly-Phe-Aib-Leu-OMe (Aib: α-amino isobutyric acid) self-assembles to a supramolecular helix through intermolecular hydrogen bonding along the crystallographic *a* axis. By contrast the β-turn structure of an isomeric tetrapeptide II, Boc-Gly-Leu-Aib-Phe-OMe self-assembles to a supramolecular β-sheet-like structure via a two-dimensional (*a*, *b* axis) intermolecular hydrogen bonding network and π-π interactions. FT-IR studies of the peptides revealed that both of them form intermolecularly hydrogen bonded supramolecular structures in the solid state. Field emission scanning electron micrographs (FE-SEM) of the dried fibrous materials of the peptides show different morphologies, non-twisted filaments in case of peptide I and non-twisted filaments and ribbon-like structures in case of peptide II.

Keywords: self-assembly; supramolecular helix; supramolecular β-sheet; peptides; filaments; ribbon

Introduction

The ability of peptides and proteins to adopt specific secondary, tertiary, and quaternary structures provides unique opportunities for the design of nanoscale materials that are not easily available with traditional organic molecules and polymers (*1*). Several reports are found where peptide based supramolecular assemblages are utilised in fabricating important nano-biomaterials (*2–9*). The design of suitable molecular building blocks, which self-assemble to form supramolecular helices (*10–14*), and β-sheets, etc. (*15–22*) is a very active area of current research. The generation of nanofibrillar structures through self-assembly of small peptides is a current field of significant research interest (*23–25*). In nature, protein chemical and conformational specificity is utilised for construction of extraordinary materials ranging from rigid, biomineralised shells and bones to high-strength spider silks (*26, 27*). Inspired by those extraordinary natural materials, we start exploring the relationship between peptide design, the resultant conformation, supramolecular structure and morphological properties of the self-assembled peptide. In this context we chose two isomeric tetrapeptides Boc-Gly-Phe-Aib-Leu-OMe (**I**) (Aib: α-amino isobutyric acid) and Boc-Gly-Leu-Aib-Phe-OMe (**II**) with alternate achiral and chiral L-amino acids (Figure 1). The incorporation of the highly helicogenic non-coded amino acid Aib was expected to provide a suitable screw conformation in the back-bone to attain a turn structure which can function as a subunit for self-assembly. Our investigation would establish whether the isomeric peptides **I** and **II** produce the same conformation and supramolecular structure and morphologically similar nano-materials through their self-assembly or differ significantly and therefore would provide insight into the mechanistic aspect of the process of self-assembly and formation of nano-biomaterials. Peptides **I** and **II** were synthesised by conventional solution phase methodology and their crystal structures were obtained by X-ray diffraction studies. The morphological features of the fibrils generated from peptide **I** and **II** in the solid state were examined by field emission scanning electron microscopy (FE-SEM).

Results and discussion

FT-IR study

The solid state FT-IR is a useful tool to get preliminary information about the peptide conformation and intermolecular hydrogen bonding. In the solid state (using KBr matrix) intense bands lying between 3382–3289 cm^{-1} have been observed for peptide **I** (3382 cm^{-1}, 3289 cm^{-1}) and **II** (3309 cm^{-1}), which indicates the presence of strongly hydrogen bonded NH groups. No band has been observed around 3400 cm^{-1} for any of the two peptides in the solid state. An absence of this band suggests that all the NHs for peptide **I** and **II** in solid state are involved in intermolecular hydrogen bonding. The CO stretching band at around 1660–1678 cm^{-1} (amide I) and the NH bending

*Corresponding author. Email: animesh_in2001@yahoo.co.in

ISSN 1061-0278 print/ISSN 1029-0478 online

DOI: 10.1080/10610270701565194
http://www.informaworld.com

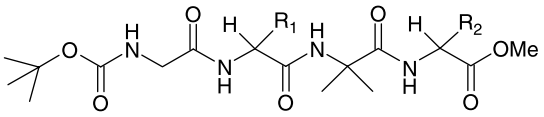

Peptide **I**: $R_1 = -CH_2Ph$, $R_2 = -CH_2CH(CH_3)_2$

Peptide **II**: $R_1 = -CH_2CH(CH_3)_2$, $R_2 = -CH_2Ph$

Figure 1. Schematic representation of peptides **I** and **II**.

and the C-N stretching peak near 1526–1532 cm^{-1} (amide II) suggest the presence of intermolecularly hydrogen bonded supramolecular β-sheet or helical conformation for peptide **I** and **II** in the solid state (*28*). In order to get detailed information about the conformations and self-assembly of the peptides single-crystal X-ray diffraction studies were carried out.

Single crystal X-ray diffraction studies

The single crystals suitable for an X-ray diffraction study of peptide **I** were grown from acetone by slow evaporation. The crystal structure of peptide **I** shows a folded conformation corresponding to a distorted type II β-turn structure with Phe(2) and Aib(3) occupying the $i + 1$ and $i + 2$ positions, respectively (Figure 2). In ideal type II β-turns, torsion angles of $\Phi_{i+1} = -60°$, $\psi_{i+1} = +120°$, $\Phi_{i+2} = +80°$, $\psi_{i+2} = 0°$ have been observed. As a consequence of deviation of $\Phi_{i+1}(-52.6°)$, ψ_{i+1} $(+132.6°)$, Φ_{i+2} $(+67.7°)$ and ψ_{i+2} $(+21.2°)$ from these values (Table 1), a weak 4 → 1 hydrogen bond between Gly(1)C═O and Leu(4)-NH with an N13 . . . O6 distance of 3.20 Å resulted. The observed hydrogen bond (H– –O═C) distance is found to be 2.46Å with an N13-H– –O6 angle of 146° (Table 2). The residues Gly(1) and Leu(4) present outside the turn region show completely extended conformation characterised by the Φ, ψ values as 132.7°, 171.6° at Gly and −113.6°, +143.2° at Leu (Table 1). In the solid state, the β-turn subunits of peptide **I** are regularly inter-linked via intermolecular hydrogen bonds and thereby form a supramolecular helix along the crystallographic ***a*** axis (Figure 3). The turns are stacked along the screw axis parallel to three independent intermolecular hydrogen bonds N4-H . . . O9 (0.5 + x, 0.5 − y, −z), N10-H . . . O3 (0.5 + x, 0.5 − y, −z) and N7-H . . . O16 (0.5 + x, 0.5 − y, −z) of 2.25 Å, 2.03 Å and 2.27 Å, respectively. The hydrogen bonding parameters are listed in Table 2. Another interesting feature is that the peptides are stacked over each other in antiparallel fashion so that a supramolecular helix is formed via these three intermolecular hydrogen bonds (Figure 3a). When the side chains of the peptide and all hydrogen atoms are omitted the helicity of the supramolecular structure becomes more apparent (Figure 3b). This finding is of particular biological relevance since supramolecular peptide-helices occur throughout living organisms with different levels of self-organization and self-association such as collagen fibers (*29*). Various chemically designed supramolecular helices have also been reported in the

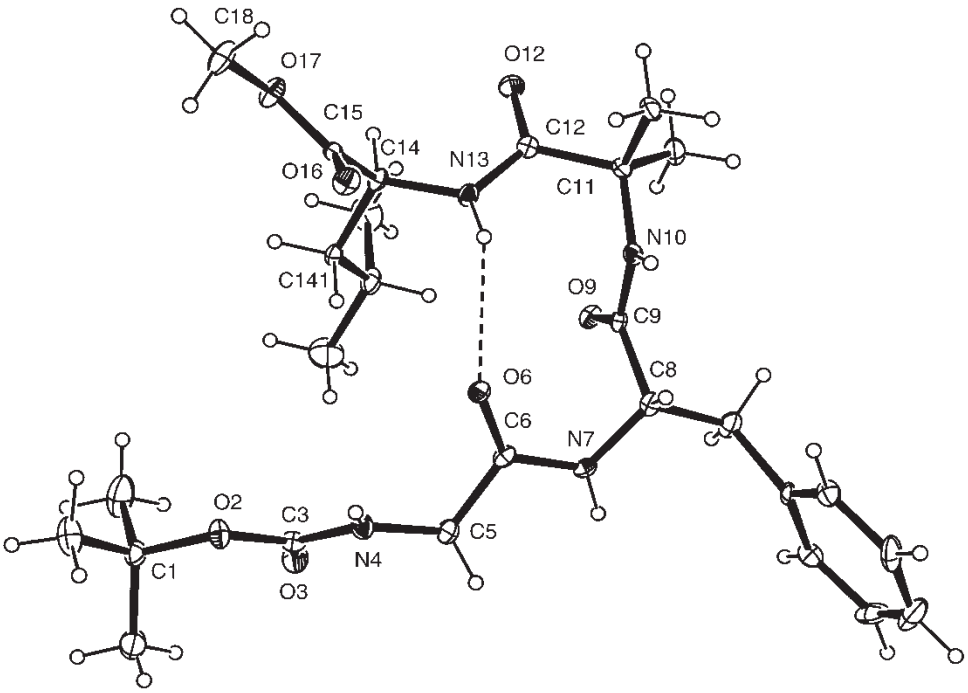

Figure 2. ORTEP diagram of the peptide **I** with atom numbering scheme. Ellipsoids are shown at 25% probability. The intramolecular hydrogen bond is shown as a dotted line.

Table 1. Selected back-bone torsion angles (deg) in peptides Boc-Gly(1)-Phe(2)-Aib(3)-Leu(4)-OMe **I** and Boc-Gly(1)-Leu(2)-Aib(3)-Phe(4)-OMe **II** (**A** and **B**)

Peptide	Residue	Φ	ψ	ω
I	Gly (1)	132.7(4)	171.6(4)	−179.0(4)
	Phe (2)	**−52.6(5)**	**132.6(3)**	−179.2(4)
	Aib (3)	**67.7(5)**	**21.2(5)**	170.0(3)
	Leu (4)	−113.6(4)	143.2(4)	178.3(4)
IIA	Gly (1)	140.7(17)	162.4(7)	−178.0(4)
	Leu (2)	**− 57.3(10)**	**127.0(6)**	155.9(12)
	Aib (3)	**50.9(7)**	**40.4(6)**	172.1(5)
	Phe (4)	−56.8(7)	136.3(5)	168.5(5)
IIB	Gly (1)	−56.5(38)	143.9(11)	165.0(17)
	Leu (2)	**− 55.4(9)**	**126.3(6)**	173.9(7)
	Aib (3)	**54.9(7)**	**41.6(7)**	174.6(5)
	Phe (4)	−63.0(7)	139.3(5)	173.0(5)

literature such as helicates of Lehn in 1987 (*30*), 2,2′-biimidazole based helix of Sessler (*31*), supramolecular helix from self-assembly of disk-shaped molecules driven by π-π stacking interactions (*32*), etc.

The single crystals of the isomeric peptide **II** were grown from $CHCl_3$-petroleum ether by slow evaporation. The crystal structure of peptide **II** reveals two independent molecules **IIA** and **IIB** in the unit cell with space-group P1. The torsion angles reported in Table 2 show that the backbone conformations are similar apart from C(3)-N(4)-C(5)-C(6) which is 140.7(17) in **IIA** and −56.6(38) in **IIB**. However both molecules adopt type II β-turns conformation with Leu(2) and Aib(3) occupying the $i + 1$ and $i + 2$ positions, respectively (Figure 4, Table 1). Like type II β-turn of peptide **I**, the type II β-turns of peptide **II** also form a weak $4 \rightarrow 1$ intramolecular hydrogen bond, with N(13)...O(6) distances of 3.26 Å and 3.24 Å in **IIA** and **IIB**, respectively (Table 2). The type II β-turn of peptide **IIA** self-assembles via intermolecular hydrogen bond between Aib(3)-NH of one molecule with Aib(3)C = O of another neighbouring molecule (N_{10A}-H−−-O_{12A}, 1 + x, y, z) to form a semi-cylindrical structure along the crystallographic *b* axis (Figure 5a, Table 2). The molecules are also packed by π-π interactions between the phenyl rings. These cylindrical structures are further connected along the *a* axis through intermolecular hydrogen bond between Leu(2)-NH of one molecule with Phe(4)-C = O of another molecule (N_{7A}-H−−-O_{16A}, 1 + x, y − 1, z) to form a two-dimensional (***a***, ***b*** axis) monolayer of β-sheet of turn **IIA** (Figure 5b, Table 2). The formation of a similar sheet-like structure with turn **IIB** is also observed in the solid state. Interestingly the β-sheets of turn **IIA** and **IIB** are stacked alternatively through van der Waals interactions in the *c* direction to form the complex quaternary sheet structure (Figure 5c). The studies clearly demonstrate that the pattern of self-assembly of the two isomeric peptides **I** and **II** in the solid state are significantly different. While peptide **I** self-assembles in one direction to create supramolecular helices, peptide **II** forms layers of β-sheets through an extensive two dimensional hydrogen bonding network and π-π interactions. It is well documented fact that π-π interactions have a significant role in amyloid aggregation (*33*).

Table 2. Intra-molecular and inter-molecular hydrogen bonding parameters of peptides **I** and **II** (**A** and **B**)

D-H−-A	H−-A/ Å	D−-A/ Å	D-H−-A/°
Peptide **I**			
N13-H...O6	2.46	3.205(4)	146
N4-H...O9[a]	2.25	3.038(5)	152
N10-H...O3[a]	2.03	2.894(4)	176
N7-H...O16[a]	2.27	3.037(4)	148
Peptide **II**			
N(13B)-H...O(6B)	2.52	3.240(9)	142
N(10B)-H...O(12B)[b]	2.08	2.909(7)	161
N(7B)-H...O(16B)[c]	2.04	2.893(7)	170
N(13A)-H...O(6A)	2.50	3.268(8)	148
N(10A)-H...O(12A)[b]	2.06	2.888(6)	161
N(7A)-H...O(16A)[d]	2.09	2.943(10)	173

Symmetry equivalents [a] 0.5 + x, 0.5 − y, −z; [b] 1 + x, y, z; [c] x, 1 + y, z; [d] 1 + x, y − 1, z

Morphological Studies

It has been suggested that not only β-sheets but also helices have a significant role in amyloid fibril formation where the α-helices are stacked along the fibril axis (*34*). Goldsbury *et al.* have suggested that, for human amylin, α-helices may have a role in highly ordered self-aggregated amyloid plaque formation (*35, 36*). Recently several reports show that supramolecular β-sheet forming small peptides promote amyloid-like fibrillation in the solid state (*15–22*). Peptide based supramolecular helices also produce fibrillar structures through self-assembly (*10–14*). Therefore, we become interested in exploring the possibility of fibril formation in peptides **I** and **II**. Field emission scanning electron microscopic (FE-SEM) images of the dried fibrous material of peptide **I** grown slowly from acetone, the same solvent from which the single crystals were grown clearly demonstrate that the aggregates in the solid state are bunches of non-twisted filamentous fibrils (Figure 6). On the other hand the FE-SEM images of the fibrous material of peptide **II** grown from chloroform-petroleum ether show the formation of both non-twisted filaments and ribbon-like structures (Figure 6).

FT-IR studies as well as crystal structure analysis reveal that two isomeric tetrapeptides self-assemble to form intermolecularly hydrogen-bonded β-sheet and helical structures. All these peptides on further self-assembly form fibrilar structure in the solid state. Peptide **I** exhibits supramolecular helix mediated higher ordered self-assembly which leads to filamentous fibril formation. Some recent reports do indicate that supramolecular helix of small

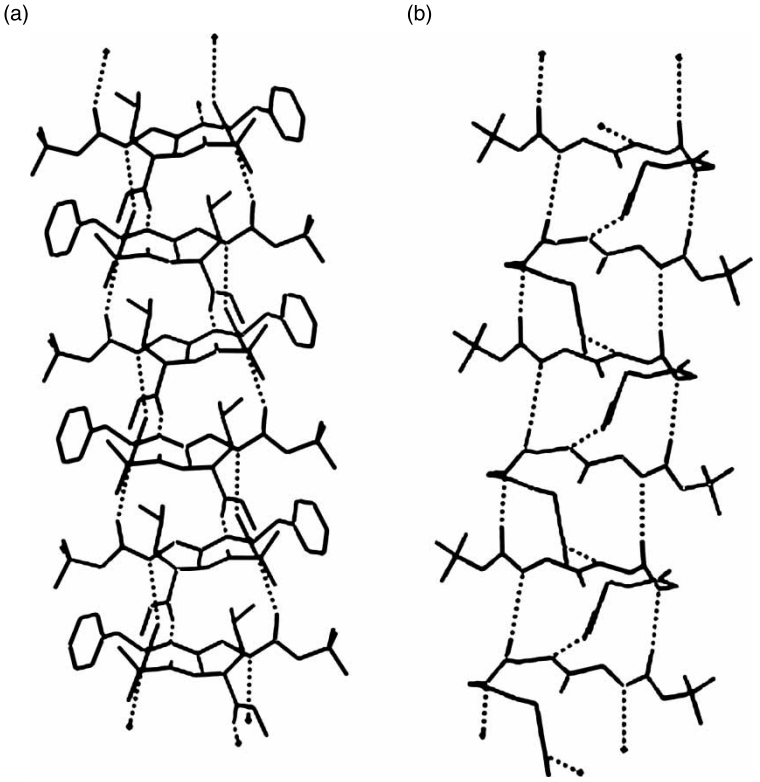

Figure 3. (a) Packing diagram of peptide **I** showing the self-assembly. There are three independent intermolecular hydrogen bonds, shown as dotted lines, connecting molecules along the ***a*** axis. (b) Packing diagram showing the formation of the supramolecular helix (side chains and hydrogen atoms are omitted for clarity, only intermolecular hydrogen bonds are shown).

peptides can promote filamentous fibrillation through higher order self-assembly (*10–14*). In the case of peptide **II**, the ribbon-like structures are formed through an extensive hydrogen bonding network of peptide **II** in the solid state. It is worth mentioning that in the amyloidogenic peptide calcitonim ribbon-like structures twist back upon themselves to afford hollow tube like assemblies (*37*).

Conclusions

Two isomeric tetrapeptides **I** and **II** have been designed incorporating highly helicogenic Aib to generate turn structures which can function as subunits in self-assembly. In the solid state the intermolecular hydrogen bond mediated self-assembly of the turn structure of peptide **I** leads to the formation of unidirectional supramolecular

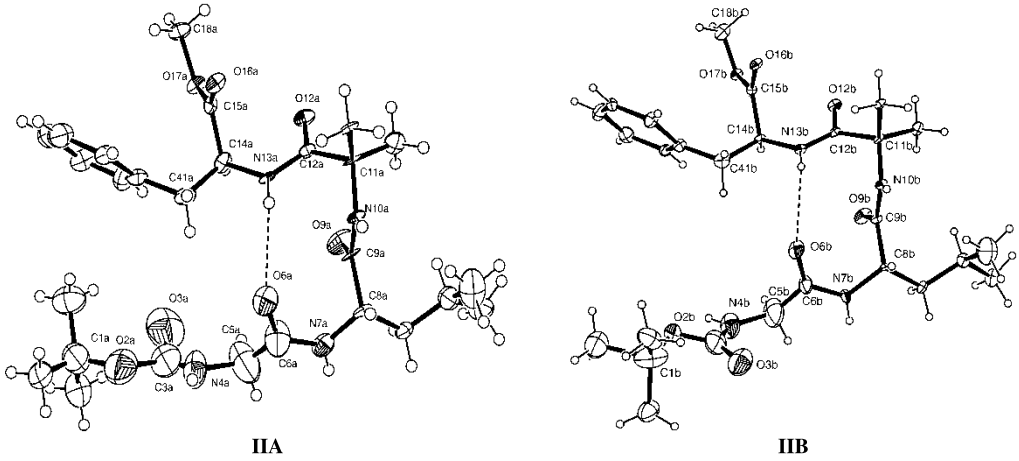

Figure 4. ORTEP diagrams of the two molecules of peptide **II** with atom numbering scheme. Ellipsoids are shown at 25% probability. The intramolecular hydrogen bonds are shown as dotted lines.

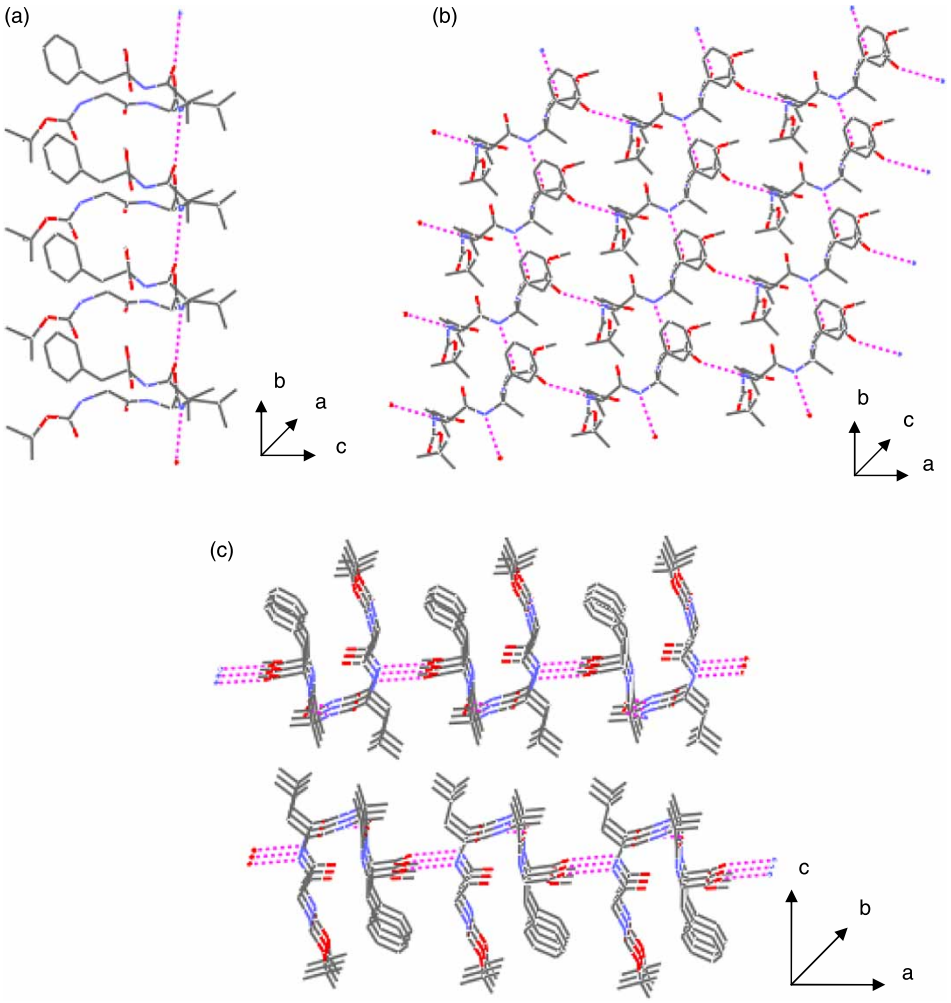

Figure 5. (a) Packing of peptide **II** showing self-assembly of turn **IIA** along the crystallographic ***b*** axis to form semi-cylindrical structure (hydrogen atoms are omitted, only intermolecular hydrogen bonds are shown); (b) Self-association of turn **IIA** along the crystallographic ***a*** axis forming two dimensional (***a***, ***b*** axis) monolayer of β-sheet. Turn **IIB** also shows similar packing; (c) The β-sheet layers of turn **IIA** and **IIB** are stacked alternatively through van der Waals interactions along the crystallographic ***c*** axis (only intermolecular hydrogen bonds are shown). It also shows the π-π interactions between the phenyl rings.

helices, whereas that of peptide **II** to a two dimensional monolayer of supramolecular β-sheet. Morphological studies with FE-SEM show that while peptide **I** generates filamentous fibrils in the solid state, the isomeric peptide **II** leads to the formation of ribbon-like structures. The present results demonstrate the importance of hydrogen bonding and pattern of self-assembly on the morphological properties of fibrillar structures. The study may help to understand the structure and function of various abnormal peptides such as prion and the Alzheimer's amyloid *etc*. and also in designing new nano-biomaterials.

Experimental

Synthesis of peptides

The peptides **I** and **II** were synthesised by conventional solution phase methods by using a fragment condensation strategy. The Boc group was used for N-terminal protection, and the C-terminus was protected as a methyl ester. Deprotection was performed by using CF_3COOH or saponification, respectively. Couplings were mediated

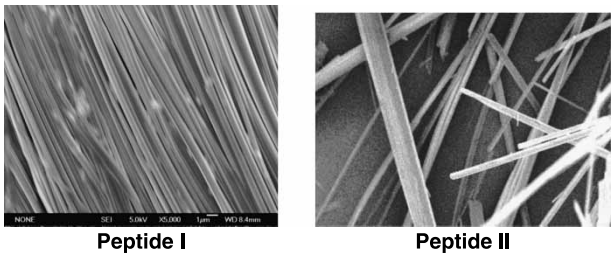

Figure 6. The FE-SEM images of the fibrous material of the peptides showing the formation of non-twisted filamentous fibrils in case of peptide **I** and filaments and ribbons in case of peptide **II**.

by dicyclohexylcarbodiimide/1-hydroxybenzotriazole (DCC/ HOBT). All intermediates were characterised by thin layer chromatography on silica gel and used without further purification. Final peptides were purified by column chromatography using silica gel (100–200 mesh) as the stationary phase and an ethyl acetate and petroleum ether mixture as the eluent. The reported peptides **I** and **II** were fully characterised by X-ray crystallography, NMR and IR.

Synthesis of the peptide I, Boc-Gly-Phe-Aib-Leu-OMe

Boc-Phe-Aib-OMe (1)

Boc-Phe-OH (2.0 g, 7.6 mmol) was dissolved in dichloromethane (DCM, 10 ml). Aib-OMe obtained from its hydrochloride (2.3 g, 15.1 mmol) was added to it, followed by DCC (2.3 g, 11.3 mmol). The reaction mixture was stirred at room temperature for 2 days. The precipitated dicyclohexylurea (DCU) was filtered. The organic layer was washed with 1 N HCl (3 × 30 mL), 1 M Na_2CO_3 solution (3 × 30 mL) and water. The solvent was then dried over anhydrous Na_2SO_4 and evaporated *in vacuo*, giving a light yellow gum. Yield: 2.4 g (87.3%).

Boc-Phe-Aib-OH (2)

Peptide **1** (2.4 g, 6.6 mmol) was dissolved in methanol (15 mL) and 2 N NaOH (3 mL) was added to it. The reaction mixture was stirred for 1 day at room temperature. The progress of reaction was monitored by TLC. After completion of reaction the methanol was evaporated. The residue was diluted with water and washed with diethylether. The aqueous layer was cooled on ice, neutralised by using 2 N HCl and extracted with ethylacetate. The solvent was evaporated *in vacuo* to give a yellow gum. Yield: 1.6 g (69.3%).

Boc-Phe-Aib-Leu-OMe (3)

Peptide **2** (1.6 g, 4.6 mmol) was dissolved in dichloromethane (DCM, 10 ml). Leu-OMe obtained from its hydrochloride (1.7 g, 9.1 mmol) was added to it, followed by DCC (1.4 g, 6.9 mmol). The reaction mixture was stirred at room temp for 3 days. The precipitated dicyclohexylurea (DCU) was filtered. The organic layer was washed with 1 N HCl (3 × 30 mL), 1 M Na_2CO_3 solution (3 × 30 mL) and water. The solvent was then dried over anhydrous Na_2SO_4 and evaporated *in vacuo*, giving a light yellow gum. Yield: 1.9 g (86.6%). ^{1}H NMR 300 MHz ($CDCl_3$, δ ppm): 7.21–7.30 (Phenyl ring protons), 6.93 (Leu NH, 1H, *d*, J = 7.08 Hz), 6.14 (Aib NH, 1H, *s*), 5.01 (Phe NH, 1H, *d*, J = 5.6 Hz), 4.53–4.57 (C^{α}H of Phe, 1H, *m*), 4.15–4.19 (C^{α}H of Leu, 1H, *m*), 3.70 ($-OCH_3$, 3H, *s*), 3.07 (C^{β}H of Phe, 2H, *m*), 1.58 (C^{β}H and C^{γ}H of Leu, 3H, *m*), 1.43 (Boc-CH_3s, 9H, *s*), 1.40 (C^{β}H of Aib, 6H, *s*), 0.94 (C^{δ}H of Leu, 6H, *m*).

Boc-Gly-Phe-Aib-Leu-OMe (I)

Peptide **3** (1.9 g, 4.0 mmol) was dissolved in CF_3COOH (6 mL) at 0 °C. After stirring at room temperature for 6 h, concentrating under reduced pressure and drying of the residue *in vacuo* yielded the crude trifluoroacetate salt (1.7 g), which was used without further purification. Trifluoroacetate salt was dissolved in CH_2Cl_2 (5 mL) and cooled to 0 °C. This was treated successively with Et_3N (till basic in litmus), HOBT (0.5 g, 4.0 mmol), a solution of the Boc-Gly-OH (0.7 g, 4.0 mmol) in CH_2Cl_2 (4 mL) and DCC (1.2 g, 5.9 mmol). The reaction mixture was stirred at room temp for 3 days. The precipitated dicyclohexylurea (DCU) was filtered. The organic layer was washed with 1 N HCl (3 × 30 mL), 1 M Na_2CO_3 solution (3 × 30 mL) and water. The solvent was then dried over anhydrous Na_2SO_4 and evaporated *in vacuo*, giving a light yellow gum. Yield: 1.8 g (84.7%). Purification was done using silica gel as stationary phase and ethyl acetate-petroleum ether mixture as the eluent. Single crystals were grown from acetone by slow evaporation and were stable at room temp. Mp = 146–148 °C; (found: C, 60.60; H, 7.85; N, 10.41% requires: C, 60.65; H, 7.92; N, 10.48%); IR (KBr): 3382, 3289, 2962, 1744, 1678, 1532 cm^{-1}; ^{1}H NMR 300 MHz ($CDCl_3$, δ ppm): 7.22–7.36 (Phenyl ring protons), 6.96 (Leu NH, 1H, *d*, J = 8.1 Hz), 6.70 (Phe NH, 1H, *d*, J = 6.9 Hz), 6.36 (Aib NH, 1H, *s*), 5.23 (Gly NH, 1H, *t*), 4.46–4.61 (C^{α}H of Leu and Phe, 2H, *m*), 3.75–3.85 (C^{α}H of Gly, 2H, *m*), 3.73 ($-OCH_3$, 3H, *s*), 3.07 (C^{β}H of Phe, 2H, *m*), 1.65 (C^{β}H and C^{γ}H of Leu, 3H, *m*), 1.47 (C^{β}H of Aib, 6H, *s*), 1.44 (Boc-CH_3s, 9H, *s*), 0.94 (C^{δ}H of Leu, 6H, *m*).

Synthesis of the peptide II, Boc-Gly-Leu-Aib-Phe-OMe

Boc-Leu-Aib-OMe (4)

Boc-Leu-OH (1.7g, 7.4 mmol) was dissolved in dichloromethane (DCM, 10 ml). Aib-OMe obtained from its hydrochloride (2.3 g, 15.1 mmol) was added to it, followed by DCC (2.3 g, 11.3 mmol). The reaction mixture was stirred at room temperature for 2 days. The precipitated dicyclohexylurea (DCU) was filtered. The organic layer was washed with 1 N HCl (3 × 30 mL), 1 M Na_2CO_3 solution (3 × 30 mL) and water. The solvent was then dried over anhydrous Na_2SO_4 and evaporated *in vacuo*, giving a light yellow gum. Yield: 2.3 g (93.2%).

Boc-Leu-Aib-OH (5)

Peptide **4** (2.3 g, 6.9 mmol) was dissolved in methanol (15 mL) and 2 N NaOH (3 mL) was added to it.

Table 3. Crystallographic data for peptides Boc-Gly(1)-Phe(2)-Aib(3)-Leu(4)-OMe **I** and Boc-Gly(1)-Leu(2)-Aib(3)-Phe(4)-OMe **II**

	Peptide **I**	Peptide **II**
Formula	$C_{27}H_{42}N_4O_7$	$C_{27}H_{42}N_4O_7$
Formula weight	534.62	534.62
Crystallising solvent	Acetone	Chloroform/Petroleum ether
Crystal colour	Colourless	Colourless
Crystal system	Orthorhombic	Triclinic
Space group	P212121	P1
a (Å)	9.318 (4)	5.822 (1)
b (Å)	14.949 (1)	9.947 (2)
c (Å)	21.037 (1)	27.456 (6)
α (^{0})	90.00	82.42 (2)
β (^{0})	90.00	86.40 (1)
γ (^{0})	90.00	73.06 (2)
Z	4	2
V (Å^3)	2930.3 (3)	1507.3 (5)
Temperature (K)	150(2)	150 (2)
μ (Mo-Kα) (mm^{-1})	0.088	0.085
$D_{calculated}$ (g cm^{-3})	1.212	1.178
R (int)	0.0878	0.0532
No of independent reflections	8431	8557
Reflections with I $>$ 2σ (I)	5138	5457
R_1 (I $>$ 2σ (I))	0.1085	0.1073
wR_2 (I $>$ 2σ(I))	0.1752	0.2788

The reaction mixture was stirred for 1 day at room temperature. The progress of reaction was monitored by TLC. After completion of reaction the methanol was evaporated. The residue was diluted with water and washed with diethylether. The aqueous layer was cooled on ice, neutralised by using 2 N HCl and extracted with ethylacetate. The solvent was evaporated *in vacuo* to give a yellow gum. Yield: 1.2 g (54.5%).

Boc-Leu-Aib-Phe-OMe (6)

Peptide **5** (1.2 g, 3.8 mmol) was dissolved in dichloromethane (DCM, 10 ml). Phe-OMe obtained from its hydrochloride (1.6 g, 7.6 mmol) was added to it, followed by DCC (1.2 g, 5.7 mmol). The reaction mixture was stirred at room temp for 3 days. The precipitated dicyclohexylurea (DCU) was filtered. The organic layer was washed with 1 N HCl (3 × 30 mL), 1 M Na_2CO_3 solution (3 × 30 mL) and water. The solvent was then dried over anhydrous Na_2SO_4 and evaporated *in vacuo*, giving a light yellow gum. Yield: 1.5 g (82.9%). ^{1}H NMR 300 MHz ($CDCl_3$, δ ppm): 7.22–7.30 (Phenyl ring protons), 7.10 (Phe NH, 1H, *d*, J = 7.8 Hz), 6.85 (Leu NH, 1H, *d*, J = 6.8 Hz), 6.61 (Aib NH, 1H, *s*), 4.81 (C^{α}H of Phe, 1H, *m*), 3.98 (C^{α}H of Leu, 1H, *m*), 3.70 ($-OCH_3$, 3H, *s*), 3.11 (C^{β}H of Phe, 2H, *m*), 1.60 (C^{β}H and C^{γ}H of Leu, 3H, *m*), 1.49 (Boc-CH_3s, 9H, *s*), 1.44 (C^{β}H of Aib, 6H, *s*), 0.94 (C^{δ}H of Leu, 6H, *m*).

Boc-Gly-Leu-Aib-Phe-OMe (II)

Peptide **6** (1.5 g, 3.1 mmol) was dissolved in CF_3COOH (5 mL) at 0 °C. After stirring at room temperature for 6 h, concentrating under reduced pressure and drying of the residue *in vacuo* yielded the crude trifluoroacetate salt (1.7 g), which was used without further purification. Trifluoroacetate salt was dissolved in CH_2Cl_2 (5 mL) and cooled to 0 °C. This was treated successively with Et_3N (till basic in litmus), HOBT (0.4 g, 3.1 mmol), a solution of the Boc-Gly-OH (0.6 g, 3.2 mmol) in CH_2Cl_2 (4 mL) and DCC (1.0 g, 4.7 mmol). The reaction mixture was stirred at room temp for 3 days. The precipitated dicyclohexylurea (DCU) was filtered. The organic layer was washed with 1 N HCl (3 × 30 mL), 1 M Na_2CO_3 solution (3 × 30 mL) and water. The solvent was then dried over anhydrous Na_2SO_4 and evaporated *in vacuo*, giving a light yellow gum Yield: 1.6 g (95.4%). Purification was done using silica gel as stationary phase and ethyl acetate-petroleum ether mixture as the eluent. Single crystals were grown from chloroform-petroleum ether by slow evaporation and were stable at room temperature. Yield: 1.6 g (95.4%). Mp = 130–132 °C; (found: C, 60.61; H, 7.88; N, 10.50% requires: C, 60.65; H, 7.92; N, 10.48%); IR (KBr): 3309, 2958, 1743, 1660, 1526 cm^{-1}; ^{1}H NMR 300 MHz ($CDCl_3$, δ ppm): 7.16–7.33 (Phenyl ring protons), 6.92 (Phe NH, 1H, *d*, J = 7.2 Hz), 6.82 (Aib NH, 1H, *s*), 6.37 (Leu NH, 1H, *d*, J = 7.5 Hz), 5.23 (Gly NH, 1H, *t*), 4.78–4.84 (C^{α}H of Phe, 1H, *m*), 4.29–4.37 (C^{α}H of Leu, 1H, *m*), 3.70–3.80 (C^{α}H of Gly, 2H, *m*), 3.72 ($-OCH_3$, 3H,

s), 3.0–3.2 ($C^{\beta}H$ of Phe, 2H, *m*), 1.60 ($C^{\beta}H$ and $C^{\gamma}H$ of Leu, 3H, *m*), 1.53 ($C^{\beta}H$ of Aib, 6H, *s*), 1.46 (Boc-CH_3s, 9H, *s*), 0.94 ($C^{\delta}H$ of Leu, 6H, *m*).

Field emission scanning electron microscopic study

The morphology of the fibrous materials of peptide **I** and **II** were investigated using field emission scanning electron microscopy (FE-SEM). For the FE-SEM study, fibrous materials of peptide **I** (grown slowly from acetone) and that of peptide **II** (grown slowly from chloroform-petroleum ether) were dried and platinum coated. The micrographs were taken in a FE-SEM apparatus (JEOL JSM-6700F).

X-ray structure analysis

For Peptide **I** and **II** all datas were collected with MoKα radiation using the Oxford Diffraction X-Calibur CCD System. The crystals were positioned at 50 mm from the CCD. 321 frames were measured with a counting time of 10s. Data analyses were carried out with the Crysalis program (*38*). The structures were solved using direct methods with the SHELXS97 program (*39*). The non-hydrogen atoms were refined with anisotropic thermal parameters. The hydrogen atoms bonded to carbon and nitrogen were included in geometric positions and given thermal parameters equivalent to 1.2 times those of the atom to which they were attached. The absolute configurations of the molecules were established from the known chiralities of the peptides. The structures were refined on F^2 using SHELXL97 (*39*). Additional crystallographic information can be found in Table 3.

Crystal data have been deposited at the Cambridge Crystallographic Data Centre, reference CCDC 626148 and 638271.

Acknowledgements

A. Dutta is grateful to the CSIR, New Delhi for offering her a Junior Research Fellowship (JRF) and A. Dutt to UGC, New Delhi for offering her a Senior Research Fellowship (SRF). The financial assistance of University of Calcutta is acknowledged. We thank EPSRC and the University of Reading, UK for funds for Oxford Diffraction X-Calibur CCD diffractometer.

References

(1) Rajagopal, K.; Schneider, J.P. *Curr. Opin. Struct. Biol.* **2004**, *14*, 480.
(2) Krejchi, M.T.; Atkins, E.D.; Waddon, A.J.; Fournier, M.J.; Mason, T.L.; Tirrell, D.A. *Science* **1994**, *265*, 1427.
(3) Aggeli, A.; Nyrkova, I.A.; Bell, M.; Harding, R.; Carrick, L.; McLeish, T.C.B.; Semenov, A.N.; Boden, N. *Proc. Natl Acad. Sci. USA* **2001**, *98*, 11857.
(4) Clark, T.D.; Buriak, J.M.; Kobayashi, K.; Isler, M.P.; McRee, D.E.; Ghadiri, M.R. *J. Am. Chem. Soc.* **1998**, *120*, 8949.
(5) Holmes, T.C.; de Lacalle, S.; Su, X.; Liu, G.; Rich, A.; Zhang, S. *Proc. Natl Acad. Sci. USA* **2000**, *97*, 6728.
(6) Brunsveld, L.; Folmer, B.J.B.; Meijer, E.W.; Sijbesma, R.P. *Chem. Rev.* **2001**, *101*, 4071.
(7) Lehn, J.M. *Angew. Chem., Int. Ed.* **1990**, *29*, 130.
(8) Moulton, B.; Zaworotko, M. *J. Chem. Rev.* **2001**, *101*, 1629.
(9) Aggeli, A.; Boden, N.; Cheng, Y. -L.; Findlay, J.B. C.; Knowles, P.F.; Kovatchev, P.; Turnbull, P.J.H.; Horvath, L.; Marsh, D. *Biochemistry* **1996**, *35*, 16213.
(10) Halder, D.; Maji, S.K.; Drew, M.G.B.; Banerjee, A.; Banerjee, A. *Tetrahedron Lett.* **2002**, *43*, 5465.
(11) Banerjee, A.; Maji, S.K.; Drew, M.G.B.; Halder, D.; Banerjee, A. *Tetrahedron Lett.* **2003**, *44*, 699.
(12) Maji, S.K.; Banerjee, A.; Drew, M.G. B.; Halder, D.; Banerjee, A. *Tetrahedron Lett.* **2002**, *43*, 6759.
(13) Haldar, D.; Drew, M.G.B.; Banerjee, A. *Tetrahedron* **2006**, *62*, 6370.
(14) Das, A.K.; Banerjee, A.; Drew, M.G.B.; Ray, S.; Haldar, D.; Banerjee, A. *Tetrahedron* **2005**, *61*, 5027.
(15) Dutt, A.; Drew, M.G.B.; Pramanik, A. *Org. Biomol. Chem.* **2005**, *3*, 2250.
(16) Kundu, S.K.; Mazumdar, P.A.; Das, A.K.; Bertolasi, V.; Pramanik, A. *J. Chem. Soc. Perkin Trans.* **2002**, *2*, 1602.
(17) Banerjee, A.; Maji, S.K.; Drew, M.G.B.; Halder, D.; Banerjee, A. *Tetrahedron Lett.* **2003**, *44*, 6741.
(18) Maji, S.K.; Haldar, D.; Drew, M.G.B.; Banerjee, A.; Das, A.K.; Banerjee, A. *Tetrahedron* **2004**, *60*, 3251.
(19) Banerjee, A.; Das, A.K.; Drew, M.G.B.; Banerjee, A. *Tetrahedron* **2005**, *61*, 5906.
(20) Das, A.K.; Manna, S.; Drew, M.G.B.; Malik, S.; Nandi, A.K.; Banerjee, A. *Supramolecular Chemistry* **2006**, *18*, 645.
(21) Ray, S.; Das, A.K.; Drew, M.G.B.; Banerjee, A. *Chem. Commun.* **2006**, *40*, 4230.
(22) Ray, S.; Drew, M.G.B.; Das, A.K.; Banerjee, A. *Supramolecular Chemistry* **2006**, *18*, 455.
(23) Lashuel, H.A.; LaBrenz, S.R.; Woo, L.; Serpell, L.C.; Kelly, J.W. *J. Am. Chem. Soc.* **2000**, *122*, 5262.
(24) Deechongkit, S.; Powers, E.T.; You, S.-L.; Kelly, J.W. *J. Am. Chem. Soc.* **2005**, *127*, 8562.
(25) Yokoi, H.; Kinoshita, T.; Zhang, S. *Proc. Natl Acad. Sci. USA* **2005**, *102*, 8414.
(26) Mann, S. *Biomineralization: Principles and Concepts in Bioinorganic Materials Chemistry*; Oxford University Press: Oxford, 2001.
(27) Vincent, J.F., Currey, J.D., Eds. *The Mechanical Properties of Biological Materials*; Cambridge University Press: Cambridge, 1980.
(28) Moretto, V.; Crisma, M.; Bonora, G.M.; Toniolo, C.; Balaram, H.; Balaram, P. *Macromolecules* **1989**, *22*, 2939.
(29) Eyre, D.R. *Science* **1980**, *207*, 1315.
(30) Lehn, J.M.; Rigault, A.; Siegel, J.; Harrowfield, J.; Chevrier, B.; Moras, D. *Proc. Natl Acad. Sci. USA* **1987**, *84*, 2565.
(31) Allen, W.E.; Fowler, C.J.; Lynch, V.M.; Sessler, J.L. *Chem. Eur. J.* **2001**, *7*, 721.
(32) Gallivan, J.P.; Schuster, G.B. *J. Org. Chem.* **1995**, *60*, 2423.
(33) Gazit, E. *FASEB J.* **2002**, *16*, 77.
(34) Arvinte, T.; Cudd, A.; Drake, A.F. *J. Biol. Chem.* **1993**, *268*, 6415.

(35) Goldsbury, C.; Goldie, K.; Pellaud, J.; Seelig, J.; Frey, P.; Müller, S.A.; Kistler, J.; Cooper, G.J.; Aebi, U. *J. Struct. Biol.* **2000**, *130*, 352.
(36) Farris, W.; Mansourian, S.; Chang, Y.; Lindsley, L.; Eckman, E.A.; Frosch, M.P.; Eckman, C.B.; Tanzi, R.E.; Selkoe, D.J.; Guénette, S. *Proc. Natl Acad. Sci. USA* **2003**, *100*, 4162.
(37) Bauer, H.H.; Aebi, U.; Haner, M.; Hermann, R.; Muller, M.; Arvinte, T.; Merkle, H.P. *J. Sruct. Biol.* **1995**, *115*, 1.
(38) Oxford Diffraction Ltd, *Crysalis*; v1; Oxford, UK, 2005.
(39) Sheldrick, G.M. *SHELXL-97*; University of Göttingen: Göttingen, Germany, 1997.